Modulation of Complement Activation and Amplification on Nanoparticle Surfaces by Glycopolymer Conformation and Chemistry

Kai Yu,[†] Benjamin F. L. Lai,[†] Jonathan H. Foley,[§] Michael J. Krisinger,[§,#] Edward M. Conway,[§] and Jayachandran N. Kizhakkedathu[†,‡,*]

[†]Centre for Blood Research and Department of Pathology & Laboratory Medicine and [‡]Department of Chemistry, University of British Columbia, Vancouver, British Columbia V6T 1Z3, Canada, [§]Centre for Blood Research and Department of Medicine, University of British Columbia, Vancouver, British Columbia V6T 1Z3, Canada, and [#]Department of Biochemistry and Molecular Biology, University of British Columbia, Vancouver, British Columbia V6T 1Z3, Canada

ABSTRACT The complement system plays an integral part of a host's innate immunity, and its activation is highly dependent on the chemistry and structure of a "foreign" target surface. We determined that the conformational state of glycopolymer chains, defined by the grafting density (chains/nm^2), on the nanoparticle (NP) surface acts as a "molecular switch" for complement activation and amplification, and the protein corona on the NP surface dictates this process. A grafting density threshold was determined, below which minimal complement activation was observed and above which substantial complement activation was detected. The glycopolymer-grafted NPs activated complement *via* the alternative pathway. The chemical structure of pendent sugar units on the grafted polymer was also an important determinant for complement activation. NPs grafted with glucose-containing polymer activated complement at a lower grafting density compared to NPs grafted with galactose-containing polymer. Analysis of complement activation products C3a and SC5b-9 followed a similar pattern. Complement activation on the NP surface was independent of particle size or concentration for a given conformational state of grafted polymer. To gain insight into a putative surface-dependent mechanism of complement activation, we determined the nature of adsorbed protein corona on various NPs through quantitative mass spectrometry. Elevated levels of two pro-complement proteins, factors B and C3, present on the NP surface grafted with glycopolymer chains at high grafting density compared to low grafting density surface, may be responsible for its complement activity. Galactose polymer modified NPs adsorbed more of the negative regulator of complement, factor H, than the glucose surface, providing an explanation for its lower level of complement activation.

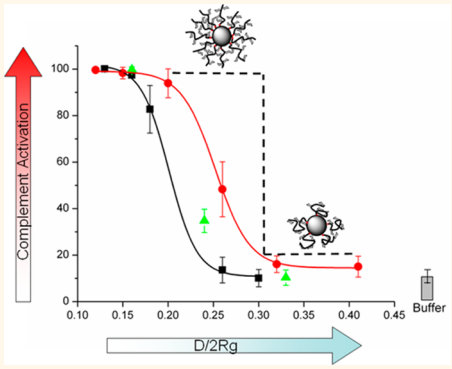

KEYWORDS: nanoparticle toxicity · complement activation · glycopolymers · surface-grafted polymers · carbohydrates · immune system

Nanoparticulate systems have found diverse applications including drug delivery, therapeutics, diagnostics, and imaging,[1−3] in which the nanoparticles (NPs) are deliberately placed inside the body. Before being delivered to specific targets in the body, NPs interact with complex protein-containing body fluids, and the resultant protein corona formed dictates the fate of the NPs.[4,5] The nature of the material and protein corona on the NP surface is thought to impact the host's immune, coagulation, and inflammatory responses and uptake of the NPs by the reticuloendothelial (RES) system.[6−7] NPs can be engineered to have different size, shape, and surface chemistry to make them suitable for specific applications. Although such modifications are known to dictate the protein corona and enhance specific targeting of the NP,[8−13] the effects of NP surface modification on the immune response are still poorly understood and warrant further study. Approved NPs have reportedly been responsible for immune-mediated hypersensitivity reactions, some of which have been unexpectedly severe, involving the central nervous system.[14] While in most circumstances, an immune response is undesirable, there are some applications

* Address correspondence to jay@pathlogy.ubc.ca.

Received for review December 23, 2013 and accepted August 8, 2014.

Published online August 08, 2014
10.1021/nn504186b

where enhanced activation of the innate immune response in concert with NP delivery might be valuable. This would be the case for immunotherapy and vaccinations. Under these conditions, complement activation induced by NPs might be beneficial by inducing dendritic cell activation, which would trigger adaptive immunity.[15,16]

As a key component of the innate immune system, the complement system consists of over 30 fluid-phase and cell-membrane-bound proteins and can be activated *via* three different initiation pathways (classical, alternative, and lectin pathways).[17] Complement allows a host to recognize and respond to foreign invaders such as bacteria, viruses, infected cells, and damaged host cells, but its activation can occur on essentially any unprotected surface. The contribution of surface functional groups, particularly high density hydroxyl groups, to complement activation has been the focus of several studies.[18−21] These have generally concluded that NPs coated with hydroxylated polymers (*e.g.*, in the form of synthetic polymers or natural polysaccharides) are safe to use *in vivo* as drug carriers, as they were found to minimally interact with components of blood and thus to evade the immune system.[18−21] In spite of these claims, the hydroxyl group is a potent nucleophile, with an ability to attack the thioester group of C3b, thereby promoting activation of complement *via* the alternative pathway.[16] Synthetic polymer carrying hydroxyl groups or natural polysaccharides such as cellulose or dextran on the surfaces activates complement *in vitro* and *in vivo*.[22−25] Complement activation by the NP surface is also dependent on the conformation and structure of polysaccharide, as well as the length of the polymer chain. Moghimi *et al*. demonstrated that NPs grafted with synthetic poloxamine enhance complement activation regardless of chain conformation, but remarkably, alteration of the chain conformation from mushroom to brush switched the initiating pathway from the classical to the lectin.[14] Other groups assessed the conformational effects of two dextran-coated NPs on complement activation and showed that NPs grafted with dextran adopting a loop conformation strongly activated complement, whereas the brush-like configuration had a less potent effect.[18,19,26,27] Finally, changing the polysaccharide structure from dextran to chitosan or dextran sulfate yielded greater protection against complement activation.[27]

Nature has created a "sugar coat" glycocalyx, which from the outer surface of the vascular endothelial cell maintains the nonthrombotic/anti-inflammatory properties of the healthy intravascular luminal wall.[28] The glycocalyx is composed of proteoglycans, glycoproteins, and glycolipids, which, as their names imply, contain large amounts of carbohydrate, consisting most prominently of amino sugars, including sialic acid, and other monosaccharide residues. The important contribution of sialic acid in suppressing complement activation *via* the recruitment of factor H has long been recognized.[29] We predicted that the architecture of sugar groups displayed on the surface (density and conformation of polysaccharides) also contributes to its anti-inflammatory properties and helps the host protect itself from complement-mediated attack. To test this hypothesis, we developed a glycocalyx mimicking system[30−32] and systematically examined the chemistry and conformation of glycopolymer chains attached with sugar residues as pendent groups (similar to glycoproteins) on the modulation and amplification of complement activation using a nanoparticulate system. Relying on surface-initiated polymerization,[30] NPs with grafted glycopolymer were prepared with good control over sugar structure and polymer chain conformation. We found that the conformation of the grafted glycopolymer structure modulates the extent of complement activation. We thus show for the first time that complement activity (initiation and amplification) can be controlled by the design of the NP surface sugar conformation. Our study provides a methodology to tune the polymer chain conformation for optimal nanoplatforms for immune system modulation. We anticipate that the structure−activity relationships between complement activation and conformational states of immobilized glycostructures can be translated for the design of surfaces for blood-contacting biomaterials used in medical devices.

RESULTS

We engineered NPs to have grafted glycopolymer layers with different chain conformation, different sugar structure, and different particle size (Scheme 1) to investigate their influence on complement activity in human serum by several well-established techniques. Sensitive hemolytic assays that quantify lysis of erythrocytes were used to measure residual total complement hemolytic activity (CH50) or alternative pathway activity (AP50), from which complement consumption by the NPs was calculated. Specific ELISAs were used to examine the activation pathways and measure the generation of C3a and the terminal membrane attack complex, SC5b-9, formed in the process of complement activation to support the hemolytic assays. To gain insights into the mechanisms underlying differential complement activation induced by the glyco-NPs, the composition of the adsorbed protein corona from human serum was determined by mass spectrometry analysis.

Synthesis of Glycopolymer Layers with Different Structure and Conformation. Glycopolymer layers (Scheme 1) refer to polymer chains carrying carbohydrate residues grafted on the NP surface. These systems provide the opportunity to mimic the cell surface glycocalyx, as sugar units are present as pendent structures along the grafted polymer chain in a manner similar

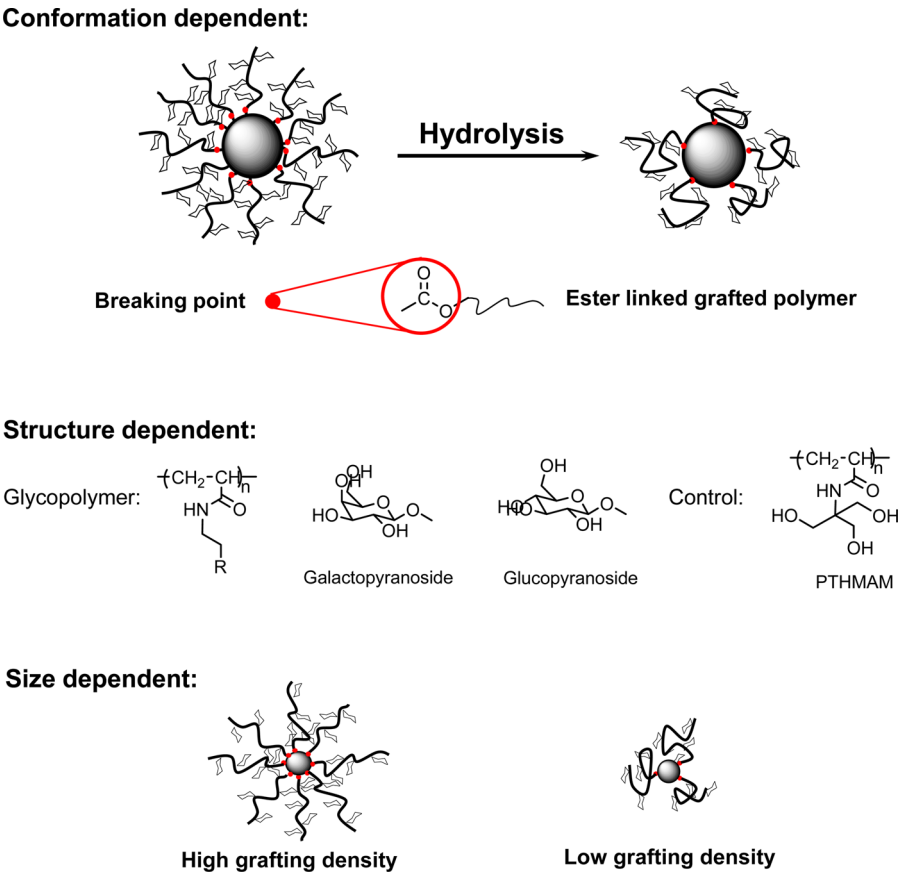

Scheme 1. Representation of glycopolymer layers with different conformation and structure on NPs of different sizes (669 and 33 nm). Glycopolymers containing galactose and glucose as pendent structures on grafted chains were used. The gradual change in the chain conformation was achieved by hydrolysis. The initiator was designed to have an ester bond in the molecular structure, which allowed the acrylamide-based polymer chains grown from the initiator to be cleaved at the breaking point

to proteoglycans present on the cell surface.[30−32] Moreover, different types of sugars could be introduced into the flexible chains to mimic oligosaccharides composed of different carbohydrate units. Glycopolymer layers carrying galactose and glucose residues were grafted onto the polystyrene (PS) NPs by surface-initiated atom transfer radical polymerization (SI-ATRP).[30,33] TEM images of glycopolymer-modified NPs revealed that the surface coating is homogeneous (Supporting Information, Figure S1). Poly(*N*-[tris-(hydroxymethyl)methyl]acrylamide) (PTHMAM) layers containing hydroxyl groups that are not arranged in the pyranose form were also synthesized as a control. The ATRP initiator was designed to have an ester bond in its structure, allowing cleavage of acrylamide-based polymer chains grown from the surface at the breaking point (Scheme 1) to generate grafted layers with different chain densities at constant molecular weight. During hydrolysis, the hydrodynamic size of particles rapidly decreased from 922 ± 58 nm in the first 2 h and then gradually over the ensuing 2 days to 747 ± 58 nm (Supporting Information, Figure S2). With careful control of hydrolysis time, glycopolymer layers with different graft densities (0.01 to 0.13 chains/nm^2) (Table 1) were synthesized for studying the influence of grafting density (consequent change in polymer chain conformation) on complement activation. Our previous study on glycopolymer grafted on substrates prepared by similar methods demonstrated that the surface coating is homogeneous for layers with different densities.[31] The grafted polymer conformation on all the NPs is still in brush conformation based on the distance between the grafted chains and the radius of gyration (R_g, measured by multiangle laser light scattering) of the chains in solution ($2R_g = 2 \times 11$ nm). The free glycopolymer chains are swollen in PBS (0.11 M), as evident from the efficient Flory exponent (v), 0.55, which is derived by fitting the dependence of R_g to the degree of polymerization (N) with the equation $R_g = aN^v$ (Supporting Information, Figure S3).[34] Tethering the chains by one end onto the NP surface further increases the degree of stretching. NPs carrying glucose moieties (Scheme 1) with similar grafting densities and molecular weight were also synthesized for the purpose of elucidating the influence of carbohydrate structure on complement activation. Characteristics of the NPs used in this study are provided in Table 1.

TABLE 1. Characteristics of Glycopolymer Brush Grafted NPs[a]

	galactose NP1	galactose NP2	galactose NP3		galactose NP4	galactose NP5
hydrolysis time	1.2 h	2.5 h	10 h	18 h	24 h	48 h
hydrodynamic size	852 ± 57 nm	822 ± 48 nm	798 ± 56 nm		769 ± 51 nm	747 ± 58 nm
grafting density (chains/nm^2)	0.13	0.085	0.064		0.031	0.023
$D/2R_g$	0.13	0.16	0.18		0.26	0.30

	glucose NP1	glucose NP2	glucose NP3	glucose NP4	glucose NP5	glucose NP6
hydrodynamic size	853 ± 52 nm	828 ± 63 nm	783 ± 47 nm	762 ± 46 nm	748 ± 62 nm	725 ± 78 nm
grafting density (chains/nm^2)	0.13	0.083	0.047	0.028	0.018	0.011
$D/2R_g$	0.12	0.15	0.20	0.26	0.32	0.41

[a] The molecular weight of the grafted galactose polymer and glucose polymer was 64 000 (PDI 1.5) and 67 000 (PDI 1.6), respectively. The molecular weight of the galactose polymer generated in solution along with grafting galactose-containing polymer on the small particles (33 nm) at concentrations of 5% and 0.6% was 110 000 (PDI 1.4) and 60 800 (PDI 4.4), respectively. The error estimate for the grafting density calculation is less than 20% of the mean value.

PTHMAM-grafted NPs have an initial hydrodynamic thickness of 804 nm, with a grafting density of 0.093 chains/nm^2. Through hydrolysis, two other samples with lower grafting densities (0.023 to 0.042 chains/nm^2) were prepared (Supporting Information, Table S1). The glycopolymer was grafted onto the smaller NPs (33 nm) by a similar SI-ATRP procedure. Two different samples with grafting densities of 0.026 and 0.17 chains/nm^2 were prepared by adjusting the monomer concentration. TEM images (Supporting Information, Figure S4) confirmed that the glycopolymer was successfully grafted onto the small NPs by measuring the change in NP size.

Influence of Glycopolymer Conformation (Grafting Density) and Carbohydrate Structure on Complement Consumption. First, we evaluated NP surface area dependent effects on complement consumption. Figure S5 (Supporting Information) shows complement consumption by NPs grafted with a glucose layer (grafting density of 0.083 chains/nm^2) as a function of surface area (the surface area refers to nanoparticles after polymer grafting; detailed calculations can be found in the Materials and Methods section). NPs of ~5 cm^2 were sufficient to induce 100% complement consumption under the conditions studied. We therefore tested samples at a surface area of 50 cm^2 to avoid any influence on results from the amount of material used. Also, in these assays, all the samples with different grafting densities were equalized by the outer surface area used to allow the NPs to have the same impact on complement activation, as the inner structure of the grafted layer may not be interacting with proteins present in serum. Also, the glycopolymer layer on the NPs surface is stable during the analysis and is not subject to enzyme hydrolysis during incubation with diluted or undiluted serum (Supporting Information, Figure S6).

We quantified the extent of complement consumption in the presence of different glycopolymer-grafted NPs. Total complement consumption (measured from a sheep erythrocyte based assay) as a function of grafting density of glycopolymers (galactose and glucose containing) on NPs with a diameter of 669 nm is shown in Figure 1A. The conformational parameter of the grafted chains, $D/2R_g$, where D is the distance between the grafted chains ($\sigma^{-1/2}$) and R_g is the radius of gyration of polymer in solution, was also calculated. The $D/2R_g$ values provide a good indication of grafted chain conformation on the nanoparticle surface.[35] A smaller $D/2R_g$ value means that the polymer chains are more closely packed and are more stretched out. Conversely, a larger $D/2R_g$ value indicates less closely packed chains that are less stretched out. As seen in Figure 1A, total complement consumption by the NPs increased dramatically with increasing grafting density. The conformation of the chains (Figure 1B) also has a profound influence on complement consumption. The conformation of the chains acts as a switch for complement consumption; that is, highly stretched chains (grafting density $\geq$0.064 chains/nm^2 or $D/2R_g$ $\leq$0.18) induce high complement consumption. Galactose glycopolymers with a grafting density of $\leq$0.031 chains/nm^2 or a $D/2R_g$ of $\geq$0.26 exhibited low complement consumption, but when the grafting density increased to >0.031 chains/nm^2, complement consumption increased dramatically.

NPs grafted with glucose-containing polymer exhibited a similar pattern to that of galactose polymer grafted NPs; however, complement consumption increased at a relatively lower grafting density. Complement consumption was minimal up to 0.018 chains/nm^2 or $D/2R_g \approx 0.32$. The control sample, *i.e.*, NPs grafted with PTHMAM, exhibited an almost identical effect on complement consumption to that of glucose-containing NPs. Soluble (ungrafted) glycopolymers, PTHMAM alone, or monomers did not induce consumption of complement, suggesting that the surface-anchoring polymer chains are essential for inducing complement activation[36] (Supporting Information, Figure S7).

To ascertain the complement-activating effects of glycopolymer-grafted NPs, we co-incubated the NP samples with normal human serum (NHS) and

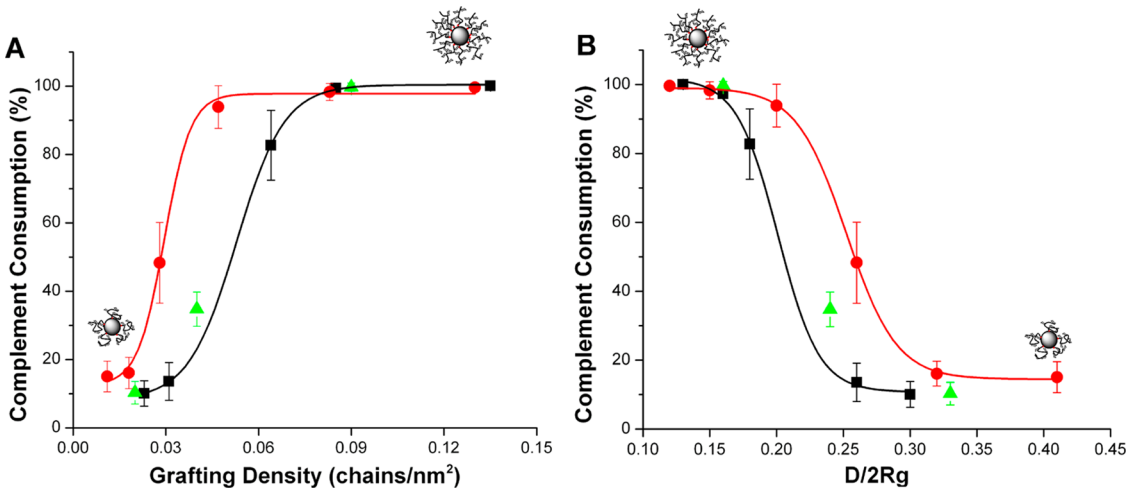

Figure 1. Dependence of complement consumption on the grafting densities (A) and conformation ($D/2R_g$) (B) upon incubation of diluted serum (0.18×) with NPs grafted with glycopolymers containing galactopyranoside (■) and glucopyranoside (red ●). Complement consumption by the control PTHMAM layer (green ▲) is also shown. Diluted fresh human serum (20%, 180 μL) was incubated with 20 μL of NP suspensions (50 cm², on 669 nm particles) for 1 h at 37 °C, and the residual total complement activity in the serum was measured using the sheep erythrocyte based hemolytic assay. Heat-aggregated IgG and EDTA (1 mM) incubated serum were used as positive and negative controls, respectively. The buffer, bare NPs, and serum have complement consumptions of 10 ± 4.5%, 8 ± 2.5%, and 9.3 ± 2.4%, respectively. Each data point represents an average ± SD (n = 5) of complement consumption in fresh serum. The curves were plotted by applying sigmoidal fitting to the measured data.

measured the residual alternative pathway activity by a rabbit erythrocyte based assay. Ungrafted glycopolymers in solution did not significantly activate complement and behaved in a similar manner to the control, *i.e.*, serum incubated in the absence of any polymer (NHS alone) (Figure 2A–C). In contrast, NPs grafted with a glycopolymer at the same concentration as the ungrafted polymer activated complement to varying degrees based on their chemical structure and chain conformation (Figure 2A–C). NPs grafted with polymer containing glucose and galactose residues or PTHMAM with grafting densities greater than 0.06 chains/nm^2 strongly activated complement, such that there was little or no measurable residual complement activity in the serum postincubation. This effect is reminiscent of zymosan, the isolated cell wall remains from yeast, which is a known complement activator and which initiates complement pathways *via* all three pathways. Indeed, in our assay, complete consumption of complement was observed with zymosan (Supporting Information, Figure S8). In addition to the markedly enhanced complement consumption induced by high grafting density surface, a striking reduction in complement consumption at a higher serum concentration (0.12×) was observed at lower glycopolymer grafting densities. For example, the extent of complement consumption was reduced from 100% to ~20% with a decrease in grafting density of galactose-containing polymer (Gal NP1 with a grafting density of 0.13 chains/cm^2 to Gal NP5 with a grafting density of 0.023 chains/nm^2, Figure 2A). The abrupt change was observed while reducing the grafting density from 0.064 to 0.031 chains/nm^2, which suppressed complement consumption from 83.2% to 40.9%, respectively (Figure 2A). A similar response was observed with the sheep erythrocyte based assay (Figure 1A).

NPs grafted with glucose-containing polymer exhibited a similar pattern of complement consumption to NPs grafted with galactose (Figure 2B). However, the extent of complement activation was stronger than with galactose-containing polymer at an equivalent grafting density (Figure 2C). NPs grafted with PTHMAM had similar effects on complement consumption as compared to the other glycopolymer-grafted NPs (Supporting Information, Figure S9). In this case, there was a notable change in complement consumption when the grafting density was reduced from 0.042 to 0.023 chains/nm^2.

Overall, the preceding experiments show that complement consumption, measured by residual erythrocyte lytic activity in diluted serum after incubation with the NPs, is dependent on the conformation and species of the carbohydrate. There is an apparent threshold grafting density (or $D/2R_g$) below which complement consumption is almost undetectable. Conversely, when grafting density exceeds that threshold, complement consumption becomes markedly elevated. Interestingly, NPs grafted with glucose-containing polymer activate complement more than NPs with galactose-containing polymer.

To further probe the pathway of complement activation brought by glycopolymer-grafted NPs with different grafting densities, we examined complement activation using sera depleted of necessary factors (C2, C1q, factor D). We selected two glucose polymer grafted NPs (Glc NP1, with 0.13 chains/nm^2, and Glc

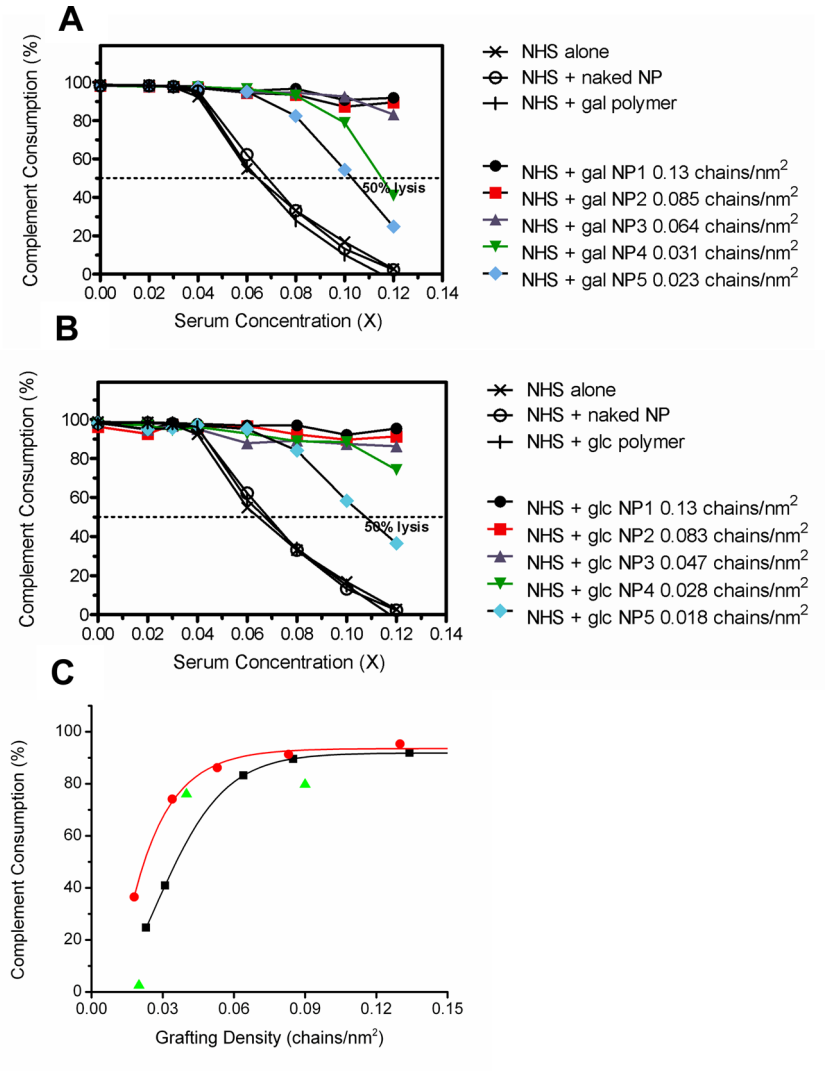

Figure 2. Effect of complement consumption measured by rabbit erythrocyte lysis upon incubation with particles grafted with glycopolymer containing galactopyranoside (A) and glucopyranoside (B) at different dilutions of human serum. Dependence of complement consumption on the grafting density of particles grafted with a glycopolymer layer containing galactopyranoside (■), glucopyranoside (red ●), and the control PTHMAM layer (green ▲) at a serum concentration of 0.12× (C). Pooled human serum (150 μL) was incubated with 100 μL of NP suspensions (150 cm^2, on 669 nm particles) for 1 h at 37 °C, and the residual complement activity of the exposed serum was measured using the rabbit erythrocyte based hemolytic assay at different serum concentrations. Zymosan and GVB-CM (GVB containing 0.15 mM Ca^{2+} and 1 mM Mg^{2+}) were used as positive and negative controls. The curves were plotted by applying sigmoidal fitting to the measured data. Results are representative of two independent experiments, each with similar results.

NP6, with 0.01 chains/nm^2), which showed distinct differences in the CH50 and AP50 analyses (high and low activation) (Figures 1 and 2). Figure 3 shows the concentration of C3a generated by incubation of the glucose polymer grafted NPs with normal human serum and deficient serum.

Incubation of Glc NP1 with normal, C2, or C1q-depleted serum resulted in similar levels of C3a generation (range: 13.6 ± 0.67 to 16.8 ± 1.6 μg/mL), suggesting that C2 and C1q of the lectin and classical or classical pathways, respectively, are not required for Glc NP1-mediated complement activation. In contrast, complement activation did not occur in factor D-depleted serum when incubated with Glc NP1 (0.32 ± 0.04 μg/mL C3a), suggesting that factor D of the alternative pathway is essential for Glc NP1-mediated complement activation.

Using the C3a generation assay, we confirmed that Glc NP6 activated complement in normal human serum (2.26 ± 1.31 μg/mL C3a) but to a much lesser degree than Glc NP1 (15.7 ± 1.27 μg/mL C3a). Activation of complement by Glc NP6 was also dependent on an intact alternative pathway since C3a was not generated in factor D-depleted serum to any appreciable extent (0.26 ± 0.04 μg/mL).

Our results indicated that the glucose polymer grafted NPs, with grafting density from 0.01 to 0.13 chains/nm^2, activated the complement system exclusively *via* the alternative pathway. The lack of effect on C3a generation by using C1q-deficient serum or

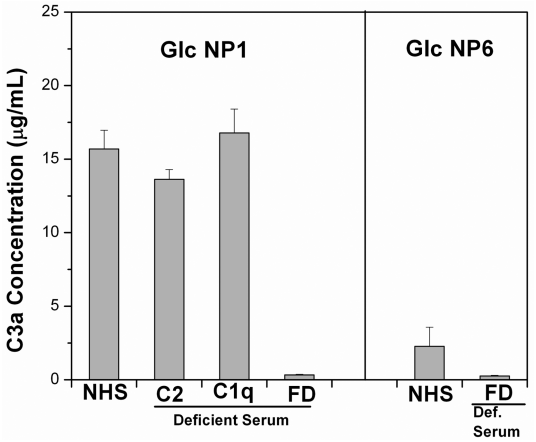

Figure 3. Generation of C3a during incubation of glucose polymer grafted nanoparticles of different grafting densities (Glc NP1 0.13 chains/nm^2, Glc NP6 0.01 chains/nm^2) with normal human serum and complement factor deficient serum. Complement activation induced Glc NP1 and Glc NP6 nanoparticles is dependent on the alternative pathway. When high-density polymer Glc NP1 was incubated in normal serum (NHS), in C2-depleted serum, or in C1q-depleted serum, complement activation, as measured by C3a generation, was similar (range: 13.6 ± 0.67 to 16.8 ± 1.6 μg/mL). When the same high-density polymer Glc NP1 was added to serum depleted of factor D, complement activation was almost entirely absent. As compared to Glc NP1, low-density polymer Glc NP6 induced significantly less complement activation in normal serum, with C3a levels reduced by >85%. However, as with Glc NP1, the presence of factor D was required for C3a generation, confirming that both polymers induce complement activation *via* the alternative pathway. Normal human serum and deficient serum (50 μL) were incubated with 20 μL of NP suspensions (50 cm^2, on 669 nm particles) for 30 min at 37 °C. C3a levels in the serum were quantified by Microvue C3a Plus ELISA.

C2-deficient serum with surface polymer conformation suggested that the classical and lectin pathways are not substantially involved. Since we observed similar behavior with galactose polymer NPs in CH50, AP50, and following complement product (C3a and SC5b-9) analysis, we inferred that NPs grafted with glycopolymer containing galactose residues also activated the complement *via* the alternative pathway.

As the complement system is activated by the alternative pathway, complement factor C3 undergoes a transesterification reaction with hydroxyl nucleophiles on the NP surface, thereby immobilizing the activation product C3b on the NP surface, with the simultaneous release of C3a peptide into the solution.[16] The attached C3b provides a surface for binding of factor B, the latter which is cleaved by circulating factor D, releasing a soluble Ba fragment. The remaining C3bBb complex is the enzymatically active C3 convertase, shifting its substrate specificity to C5, as more C3b associates with the C3bBb (yielding the C5 convertase, C3bBbC3Bb). Cleavage of C5 by the C5 convertase causes release of the soluble C5a and generation of C5b, which binds sequentially to C6, C7, C8, and multiple C9 molecules to form the terminal C5b-9 membrane-attack (MAC) complex.[14,17] To confirm the results of the hemolytic assays that quantified residual complement activity in NPs exposed to human serum, we measured the generation of C3a and terminal complex SC5b-9 in undiluted serum (Figure 4).

The influence of grafting density and conformation ($D/2R_g$ values) for galactose-, glucose-, and PTHMAM-grafted NPs on the amount of C3a generated is shown in Figure 4A and B. Glycopolymer-grafted NPs enhanced C3a levels to different extents (4.5−29 μg/mL) (depending on the grafting density) compared to the unmodified NPs (0.6 ± 0.1 μg/mL) and serum alone (1.9 ± 0.1 μg/mL). C3a levels with the NPs were higher than with free polymer (0.9−2.8 μg/mL), indicating that the increase is largely dependent on the surface. Moreover, the amount of C3a generated is clearly dependent on the conformation of the grafted chains (Figure 4B) for galactose- and glucose-containing polymer grafted NPs. Thus, the stretched chain conformation (lower $D/2R_g$ values) due to close grafting yielded higher C3a levels. Unlike PTHMAM-grafted particles, which yield an almost linear increase in C3a levels on grafting density (or a linear decrease of C3a level on the $D/2R_g$), NPs grafted with galactose- and glucose-containing polymers yielded a sigmoidal pattern, consistent with what was observed with the previous erythrocyte assays (Figures 1 and 2). Thus, when the grafting density was lower than 0.031 chains/nm^2 ($D/2R_g$ higher than 0.26), there was no appreciable increase in C3a. With grafting densities of 0.031 to 0.085 chains/nm^2 ($D/2R_g$ value between 0.16 and 0.26), the amount of C3a generated showed a sharp increase until it reached a plateau. Finally, above 0.085 chains/nm^2 ($D/2R_g$ value lower than 0.16), the amount C3a generated almost reached an elevated plateau.

Although all the NPs tested were at a similar surface area and amount of grafted polymer, the galactose and glucose NPs generated considerably more C3a than PTHMAM layers, suggesting that at comparable grafting densities C3 convertase assembly on the glucose and galacotse NPs is different than on the PTHMAM layer. Furthermore, glucose NPs yield more C3a than galactose NPs at comparable grafting densities.

We also examined the amount of SC5b-9 complex generated in undiluted human serum in the presence of different NPs (Figure 4C and D). Unmodified PS NPs generated similar amounts of SC5b-9 (0.8 ± 0.1 μg/mL) to that found in normal serum alone (0.7 ± 0.1 μg/mL). NPs grafted with glycopolymers generated significantly higher amounts of SC5b-9 in a grafting density- and conformation-dependent manner. This is again in line with the previous findings of effects on complement consumption using the erythrocyte hemolytic assays (Figures 1, 2). Notably, glucose NPs again generated more SC5b-9 complex compared to the galactose layer at comparable grafting density or $D/2R_g$ values. Also, the SC5b-9 level for all the NPs showed

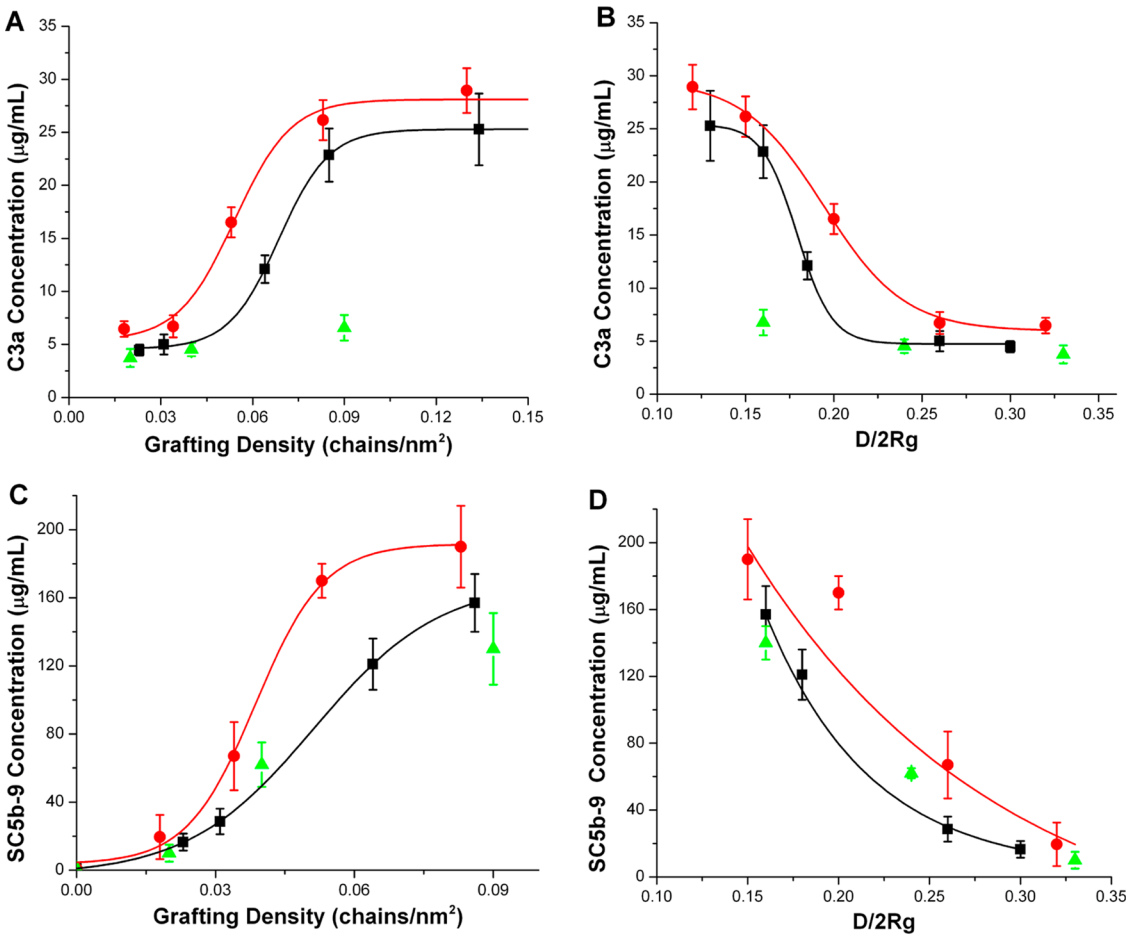

Figure 4. Dependence of the level of C3a on the grafting densities (A) and $D/2R_g$ values (B) of a glycopolymer layer containing galactopyranoside (■), glucopyranoside (red ●), and the control PTHMAM layer (green ▲). Dependence of the level of SC5b-9 on the grafting densities (C) and $D/2R_g$ values (D) upon incubation of serum with particles grafted with a glycopolymer layer containing galactopyranoside (■), glucopyranoside (red ●), and the control PTHMAM layer (green ▲). Fresh human serum (180 μL) was incubated with 20 μL of NP suspensions (50 cm^2, on 669 nm particles) for 1 h at 37 °C. C3a and SC5b-9 levels in the serum were quantified by Microvue C3a Plus and MicroVue SC5b-9 Plus ELISAs. Each data point represents an average ± SD (n = 3) of complement activation product, C3a and SC5b-9, produced in fresh serum. The curves were plotted by applying sigmoidal fitting (A, B, C) and an exponential decay function (D) to the measured data.

a rapid decay (Figure 4D) as the $D/2R_g$ value increased from 0.15 to 0.32 (the conformation changed from close packing to lose packing). Taken together, the results from the hemolytic assays and complement activation products data reveal that a delicate change in conformation or chemistry of carbohydrate structure on the NP surface significantly influences complement activation.

Influence of Particle Size on Complement Activation. Since particle size (or curvature) is likely to influence the species of surface-bound proteins when the curvature approaches the size of proteins,[37] we predicted that NP size would also influence complement protein binding and regulate the effector functions of these proteins.[38] The manner in which complement proteins bind to the NP surface as a function of particle size may also contribute to either inhibition or activation of the complement system.[8] Hence, we investigated the influence of particle size on complement activation induced by glycopolymer-grafted NPs. Galactose polymer layers with two different grafting densities were grown on the NPs having two sizes (33 and 669 nm with curvatures of 0.027 and 0.0015 nm^{-1}, respectively). As the radius of gyration of the glycopolymer (11 nm) is considerably smaller than the size of nanoparticles (33 and 669 nm), we do not expect considerable changes in polymer chain conformation with different sized particles used.[39,40] Despite the differences in NP size, the lower grafting density NPs resulted in lower complement consumption, which was not significantly different from buffer or NP control (Figure 5). NPs grafted with a galactose-containing polymer layer with higher grafting density on both NPs produced strong complement activation (>90% complement consumption measured by sheep erythrocyte hemolytic assay) (Figure 5). A similar trend was observed in the generation of C3a and SC5b-9 complex for the different sized NPs (Supporting Information, Figures S10 and 11). A loosely grafted galactose layer caused significantly less complement activation than densely grafted layers.

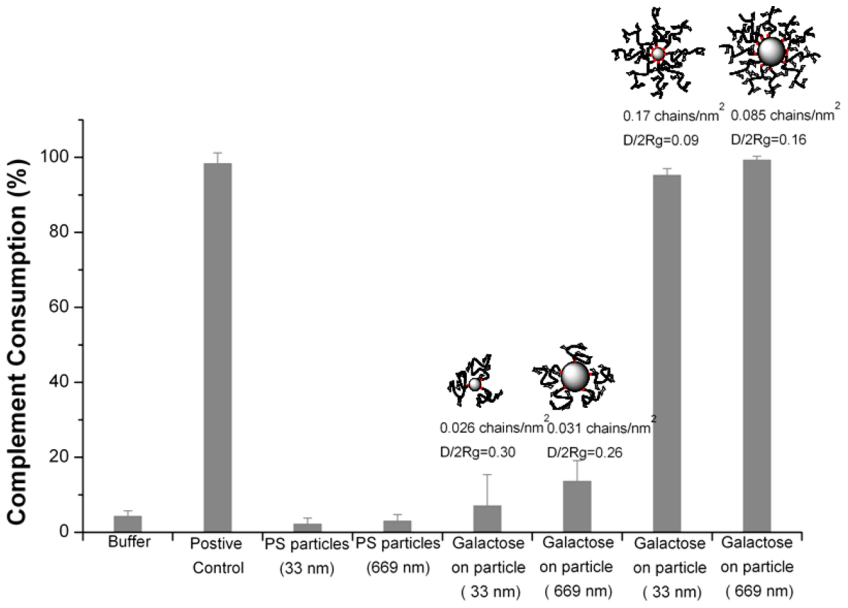

Figure 5. Effect of particle size (/surface curvature) on complement consumption (evaluated by the sheep erythrocyte based hemolytic assay) induced by NPs grafted with galactose-containing glycopolymer at two different grafting densities. Diluted fresh human serum (20%, 180 μL) was incubated with 20 μL of NP suspensions (50 cm^2, on 33 and 669 nm particles) for 1 h at 37 °C, and the residual total complement activity of the exposed serum was measured using the sheep erythrocyte based hemolytic assay. Each data point represents an average ± SD (n = 3) of three experiments (three donors) in fresh serum.

The hemolytic data together with the C3a and SC5b-9 results indicate that the curvature of the surface may not restrict C3b deposition, assembly of alternative pathway convertase, and amplification of the system. These results further demonstrate that the grafting density of the glycopolymer layer and/or polymer chain conformation on the NP surface are the determining parameters in modulating complement activation, more so than the particle size or curvature.

Influence of Particle Concentration on Complement Activation. Since some of the glycopolymer inside the grafted layer has limited access to the serum proteins, the NPs were standardized by the outer surface area to ensure that they interact with serum proteins equally. By this approach, the amount of polymer grafted on the NPs will be different, as more glycopolymer (carbohydrate units) will be present on NPs with higher grafting density. To differentiate the influence of polymer concentration and the grafting density, we investigated the effect of the concentration of glycopolymer-grafted NPs on complement consumption at a constant amount of serum (Figure 6). We used galactose polymer grafted NPs (0.031 chains/nm^2), which causes relatively low complement consumption in the hemolytic assay (Figure 1A), and galactose NPs with 0.064 chains/nm^2, which strongly activated complement. The amount of NPs used for the experiment was tripled (~150 cm^2). Thus, the amount of glycopolymer present on the NPs with a low grafting density of 0.031 chains/nm^2 at 150 cm^2 was ~1.5-fold higher than the NPs with 0.064 chains/nm^2 at 50 cm^2. The 3-fold increase in concentration of NPs with a grafting

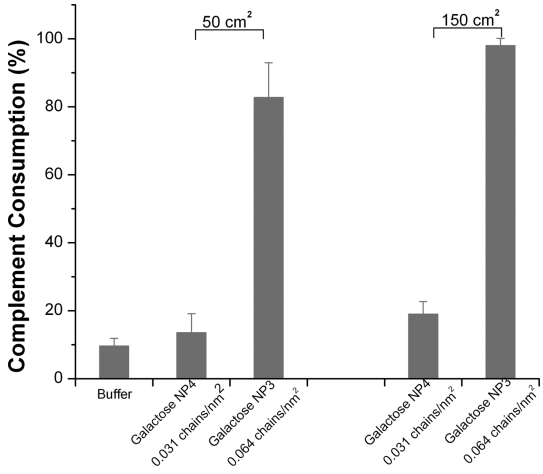

Figure 6. Influence of carbohydrate concentration (/surface area) on complement consumption of NPs grafted with glycopolymers. Two different graft densities of polymer chains were used. Diluted fresh human serum (20%, 180 μL) was incubated with 20 μL of NP suspensions (50 and 150 cm^2, on 669 nm particles) for 1 h at 37 °C, and the residual total complement activity of the exposed serum was measured using the sheep erythrocyte based hemolytic assay. Each data point represents an average ± SD (n = 3) of three experiments (three donors) in fresh serum.

density 0.031 chains/nm^2 (50 cm^2 to 150 cm^2) induced a small change (~5.4%) in complement consumption as measured by the hemolytic assay (Figure 6) and enhanced the generation of SC5b-9 by 0.6-fold (Supporting Information, Figure S12), which is much lower than the particles with higher grafting density. Overall, complement activation on surface-grafted NPs is dependent more on the conformation of the chains independent of the quantity of the NPs.

TABLE 2. List of the 20 Most Abundant Proteins Detected in the Corona on the Glycopolymer Layer with Different Grafting Density and Structure[a]

galactose layer (0.064 chains/nm^2)		galactose layer (0.031 chains/nm^2)		glucose layer (0.034 chains/nm^2)	
protein	abundance (%)	protein	abundance (%)	protein	abundance (%)
complement C3	19.20	complement C3	13.93	complement C3	15.28
apolipoprotein A-I	9.03	apolipoprotein A-I	12.37	apolipoprotein A-I	14.61
apolipoprotein E	6.21	apolipoprotein E	7.43	apolipoprotein E	11.47
serum albumin	4.80	apolipoprotein C-I	6.58	apolipoprotein C-I	6.22
apolipoprotein C-I	4.60	serum amyloid A-1 protein	3.28	serum albumin	3.51
complement component C9	3.80	apolipoprotein A-IV	3.21	apolipoprotein A-IV	3.34
serum amyloid A-1 protein	3.37	complement component C9	3.03	complement component C8 gamma chain	3.30
apolipoprotein A-IV	3.00	apolipoprotein C-III	2.59	complement component C9	3.28
apolipoprotein C-III	2.66	serum albumin	2.57	isoform 2 of clusterin	2.74
apolipoprotein A-II	2.23	keratin, type II cytoskeletal 1	2.36	keratin, type II cytoskeletal 1	2.23
complement C5	2.00	complement component C8 gamma chain	2.36	Ig lambda-2 chain C regions	2.03
Ig gamma-1 chain C region	1.88	isoform 2 of clusterin	2.29	keratin, type I cytoskeletal 9	1.96
isoform 2 of clusterin	1.65	prothrombin	2.23	Ig kappa chain C region	1.95
keratin, type II cytoskeletal 1	1.51	Ig gamma-1 chain C region	1.59	apolipoprotein C-III	1.71
vitronectin	1.48	apolipoprotein C-IV	1.47	vitronectin	1.66
Ig kappa chain C region	1.37	retinoic acid receptor responder protein 2	1.45	complement C5	1.60
Ig kappa chain V-IV region Len	1.23	vitronectin	1.44	serum amyloid A-1 protein	1.59
Ig heavy chain V-III region VH26	1.23	complement C5	1.42	prothrombin	1.35
complement component C8 gamma chain	1.19	apolipoprotein A-II	1.40	apolipoprotein C-II	1.33
complement component C6	1.16	apolipoprotein C-II	1.40	keratin, type II cytoskeletal 2 epidermal	1.28

[a] The absolute protein abundance in proteomics was estimated with the exponentially modified protein abundance index through HCD fragmentation. Protein abundance (mol %) = emPAI/$\sum$(emPAI) $\times$ 100.[52] Protein score 50 was taken as the identity threshold as the confidence level is higher than 95%. The full list of identified proteins is provided in the Supporting Information (Tables S2, S3, S4).

Mechanism of Modulation of Complement Activation by Grafted Glycopolymer Chains Evaluated by Mass Spectrometry. Because complement protein, especially complement C3, is chemically fixed on the particle during complement activation, we suppose that analysis of the hard corona (including composition and organization orientation of the corona),[41−44] which is the biological identity of the nanoparticles, would be important to explicitly understand the mechanisms. We first investigated the composition of the adsorbed protein corona on NPs from human serum by quantitative mass spectrometry (MS) based proteomics analysis. Two approaches were used: (a) Semiquantitative data regarding the protein corona on NPs were obtained by analyzing the trypsin-generated peptides.[33] (b) Relative quantification of the protein corona on two different NPs was performed (binary analysis) by chemical dimethylation of peptides using either light (CH_2O) or medium (CD_2O) isotopologues of formaldehyde.

Two sets of NPs were used for the experiments. In the first set, we used galactose-containing polymer grafted NPs with graft densities 0.031 and 0.064 chains/nm^2 to investigate the mechanisms by which the conformation of grafted chains affects complement activation. In the second set, galactose- and glucose-containing polymer grafted NPs at a similar grafting density (0.03 chains/nm^2) were compared to determine the influence of carbohydrate structure.

Table 2 lists the 20 most abundant proteins detected on NPs. The list of other identified proteins is provided in the Supporting Information (Tables S2, S3, S4). Notably, as seen in Table S2, for all the NPs tested, proteins involved in the classical and lectin pathways of complement activation, including C4 and C1, were not abundant in the protein corona (less than 0.1 mol %), evidence that the glycopolymer-grafted surface activates complement *via* the alternative pathway. Complement protein C3 was the major adsorbate on the surface (14−19%). This was followed by the different apolipoproteins (including A-I (9−15%), A-IV (3%), C−I (5−7%), C−III (2−3%), and E (6−11%)) and serum albumin (3−5%), which are adsorbed onto the particles nonspecifically. To examine the influence of nonspecific protein adsorption on NPs, we used two different experimental approaches: (1) the NPs were incubated with C3-depleted serum (undiluted), and we measured the total amount of adsorbed proteins. Since the NPs activated complement exclusively through the alternative pathway (Figure 3), this allowed the measurement of nonspecific protein adsorption in serum (Supporting Information, Table S5). (2) We also examined the nonspecific protein adsorption by incubating the NPs in single protein solution (human serum albumin (HSA)). Table S5 (Supporting Information) shows the adsorbed protein amount in the desorbed solution on different galactose polymer grafted NPs and bare NPs. The galactose NPs, which showed distinguishable complement

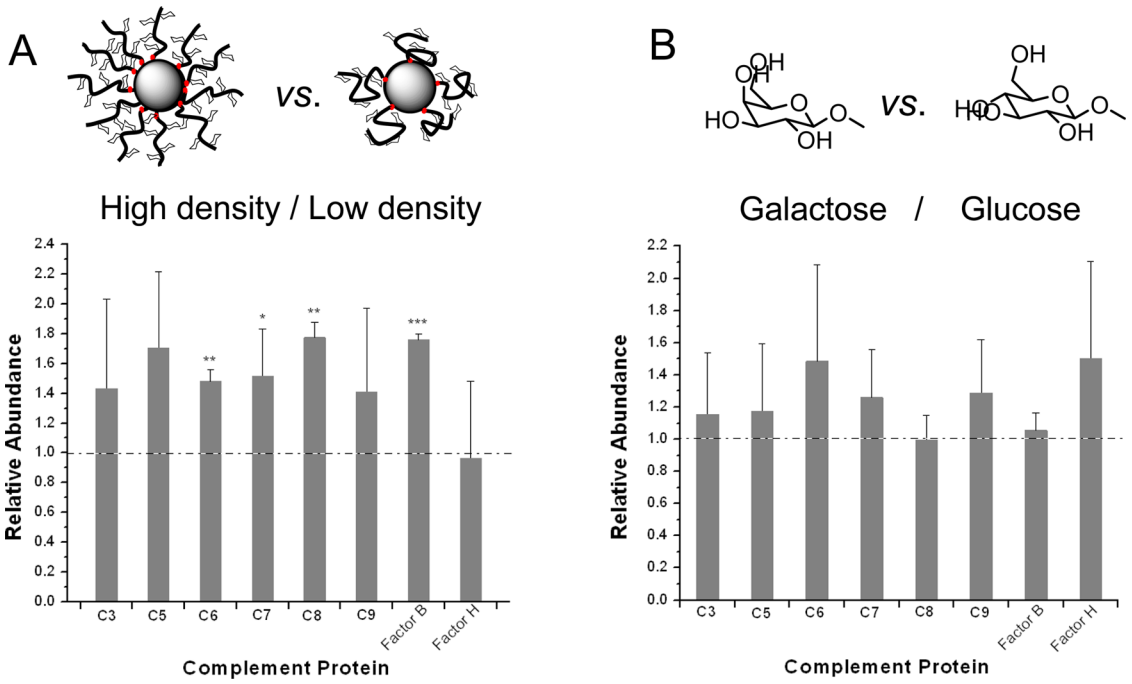

Figure 7. Comparison of abundance of complement proteins on glycopolymer-grafted NPs from serum determined by mass spectrometry-based proteomic analysis. For proteome profiling by relative quantification, binary analysis was performed by chemical dimethylation of peptides using either light (CH_2O) or medium (CD_2O) isotopologues of formaldehyde. (A) Influence of conformation of glycopolymer layer. Relative abundance of complement proteins adsorbed onto the galactose layer having grafting a density of 0.064 chains/nm^2 to the samples having 0.031 chains/nm^2. (B) Influence of chemistry of glycopolymer structure. Relative abundance of complement proteins adsorbed onto the galactose layer with a grafting density of 0.031 chains/nm^2 to the glucose layer with a similar density (0.034 chains/nm^2). *$p < 0.05$, **$p < 0.005$, ***$p < 0.0005$. Comparison is made between relative abundance of complement proteins. Glycopolymer-grafted PS nanoparticles (45 μL, 113 cm^2) were incubated with 405 μL of fresh human serum at 37 °C for 1 h, after which the nanoparticles were washed three times with 180 μL of PBS buffer. The NP suspension was then subject to MS analysis. Results are representative of two independent experiments, each with similar results. Proteins with ion scores higher than threshold value indicate their identity with confidence greater than 95%. Ion scores for complement proteins are listed in Tables S6 and S7 in the Supporting Information.

consumption (galactose NP3, NP5; Figure 1), showed only a small difference in nonspecific protein adsorption (0.02−0.03 mg/mL) in C3-depleted serum or HSA solution. We assume that such a small difference in nonspecific protein adsorption is unlikely to induce dramatic differences in complement activation as shown here. The bare NPs, which showed greater nonspecific adsorption, did not initiate complement activation.

Since the relative abundance of other complement proteins was not sufficient to allow a comparison between the two sets of NPs, an isotopic labeling method was used (Figure 7A). Adsorption of C3 on the high grafting density surface (0.064 chains/nm^2) was 1.4-fold greater than on the surface with low grafting density (0.031 chains/nm^2). The relative abundance of C3 on the NP surface determined by MS correlates with the C3a levels in the supernatant solution (Figure 4A and Figure 7A), suggesting that the C3 bound on the NPs is most likely in the form of either C3b or iC3b.[24]

We also found that the relative amount of factor B, a complement-activating factor in the alternative pathway, was detected on the galactose polymer NP with high grafting density and was 1.7-fold higher than on the NP with low grafting density (Figure 7A). Relative amounts of factor H were not different on these NPs. All other proteins in the terminal pathway of complement (C5, C6, C7, C8, and C9) were present in excess on the NP surface with high grafting density, more so than on the surface with low grafting density.

We also analyzed the protein corona present on galactose and glucose polymer grafted NPs with similar grafting densities (0.03 chains/nm^2) and $D/2R_g$ values (Figure 7B). Although the amount of C3 and factor B present on the galactose layer was slightly higher than on the glucose layer, the galactose layer recruited more factor H (1.6-fold higher).

DISCUSSION

Engineering the NP surface chemistry to modulate the immune system response is important not only to various clinical applications but also for improving the stability and biocompatibility of NPs as drug carriers and for other applications. Previous studies have shown

that complement activation on surfaces grafted with polysaccharides and polymers containing hydroxyl groups is reduced by increasing the grafting density of chains.[18,19,26,27] For example, Labarre *et al*. observed that complement activation (evaluated by cleavage of C3) by the polysaccharide bound in the "loops" conformation (low grafting density) was higher than that of the polysaccharide in the brush regime (high grafting density).[27] Iwata *et al*. came to similar conclusions when examining the complement activation induced by poly(vinyl alcohol)-grafted surfaces in serum.[26] These results were explained by the steric repulsion of proteins brought by brush conformation, which limits the access of C3 to the surface, while helping the complement regulatory factor H access its binding site on C3b. However, our hemolytic and complement activation product analyses indicate that glycopolymer-grafted NPs with high grafting density (densely grafted surfaces with lower $D/2R_g$ values) considerably increased complement activation. The NP surface grafted with low grafting density of glycopolymer chains (loosely grafted surfaces with higher $D/2R_g$ value) dampened complement activation. There is an apparent threshold grafting density (or $D/2R_g$) below which complement consumption is almost undetectable. Conversely, when grafting density exceeds that threshold, complement consumption becomes markedly elevated. To address this contradiction and to understand the glycopolymer conformation dependent complement activation by NPs, we investigated the composition of the adsorbed protein corona on NPs by quantitative MS based proteomics analysis. By determining the relative abundance of certain complement proteins on the surface of NPs with different conformations (grafting density) and structures, this approach provided some insights into potential mechanisms by which complement activation was differentially modulated. However, the biophysical and molecular mechanisms by which the grafted NPs actually activate the alternative pathway need further characterization.

Factor B and factor H are two key serum proteins involved in complement activation and regulation.[17,29] In the alternative pathway, the binding of factor B to surface-attached C3 (H_2O) is required for subsequent cleavage of factor B to Ba and Bb and the generation of the C3 convertase (C3bBb). This is a critical step in the amplification of the complement cascade on surfaces carrying hydroxyl or amine groups.[36,45] Factor H, a soluble protein present in serum, is a negative regulator of complement activation. In association with factor I, it binds to C3 convertase and inactivates the amplification loop.[29,46] The differences in surface association of these proteins could potentially influence complement activation and amplification. In our MS analysis, we concentrated on the analysis of the hard protein corona on the surface of NPs; however this will not provide evidence for the weakly interacting proteins or proteins that are washed away during the sample preparation. Future analysis of the soft protein corona,[41−44] although difficult, on the NP surface will hopefully uncover important roles of other proteins in serum on differential complement activation and fixation by glycoNPs.

Densely grafted galactose polymer NPs carry a higher density of hydroxyl groups on the surface, thereby favoring recruitment of C3b. The surface with a low grafting density recruited less factor B and had a similar amount of decay factor H, resulting in dampening of complement activation (Figure 7). The hemolytic assays (Figures 1, 2) and measures of the generation of C3a and SC5b-9 indicate that an optimal carbohydrate density or chain conformation is crucial for the amplification step to occur. The conformation of glycopolymer chains on NP appears to play a critical role as an *on*−*off* switch for surface-induced complement activation.

Finally and somewhat surprisingly, NPs grafted with glucose-containing polymer appear to activate complement more than NPs with galactose-containing polymer. The recruitment of more factor H, revealed by the MS studies (Figure 7B), may contribute to this by interfering with formation of or destabilizing the C3 convertase on the galactose layer, thereby suppressing complement activation. The mechanism of recruitment of more factor H on the galactose surface requires further investigation.

CONCLUSIONS

NPs grafted with glycopolymer containing different carbohydrate residues were prepared by surface-initiated polymerization. Through subsequent hydrolysis, the conformation of grafted glycopolymer chains on the NP surface was altered by gradual change of the grafting density of polymer chains. We determined that the grafting density and conformation of the chains acted as a "molecular switch" for complement activation. Above a threshold grafting density, NPs induced substantial complement activation, whereas minimal activation was observed below that threshold grafting density. NPs grafted with glucose-containing polymer were stronger activators of complement than NPs grafted with galactose-containing polymer. Adsorption studies revealed that NPs grafted with glycopolymer chains at high density accumulated more factor B and C3, findings which were consistent with higher complement activation induced by these NPs. Differences between complement activation induced by glucose- and galactose-containing NPs may be attributed to differential surface binding of factor H. Particle size and concentration exhibited minimal effects on complement activation. These new insights into how complement activation is differentially altered by glycopolymer conformation

and carbohydrate chemistry may ultimately be useful in the design of safer and more effective blood-contacting biomaterials, NPs for drug delivery, and/or immunotherapies.

MATERIALS AND METHODS

Materials. 2′-Acrylamidoethyl-β-D-galactopyranoside and 2′-acrylamidoethyl-β-D-glucopyranoside were synthesized following our previously published procedure.[32] Atom transfer radical polymerization (ATRP) initiator modified polystyrene particles with two different sizes (33 and 669 nm, respectively) were synthesized by a shell growth mechanism utilizing surfactant-free emulsion polymerization of styrene and 2-(methyl 2′-chloropropionato)ethyl acrylate.[47] Pristine PS NPs with a diameter of 27 nm (10% solid content) were purchased from Bang Laboratories Inc. (IN, USA). 2-Hydroxyethyl acrylate (96%), 2-chloropropionyl chloride (97%), Cu(I)Cl (99%), Cu(II)Cl_2 (99%), and tris[2-(dimethylamino)ethyl]amine (Me_6TREN) were purchased from Sigma-Aldrich (ON, Canada).

Grafting of Glycopolymer Layers with Different Conformation and Structure. Two different sized PS particles (33 ± 6.7 and 669 ± 6.3 nm) and two monomers, 2′-acrylamidoethyl-β-D-galactopyranoside and 2′-acrylamidoethyl-β-D-glucopyranoside, were used. Glycopolymer structures on these NPs were synthesized by SI-ATRP.[30]

Grafting of Glycopolymer Layers onto Particles with a Diameter of 669 nm. Initiator-modified PS particles (60 mg), nonionic surfactant Brij 35 (3.3 mg), and Milli Q water (2 mL) were added successively into a glass tube, which then was degassed by three freeze−pump−thaw cycles. The PS particles were dispersed in the water homogeneously by subjecting the tube to ultrasonication for 15 min before transferring to the glovebox. In another glass tube, CuCl (6 mg), $CuCl_2$ (1.3 mg), and Me_6TREN (72 μL) were added successively followed by the addition of Milli Q water (6.5 mL). The glass tube was degassed by three freeze−pump−thaw cycles and transferred to the glovebox. 2′-Acrylamidoethyl-β-D-galactopyranoside (100 mg) was added to the prepared solution (1 mL). After the monomer was dissolved, the solution was mixed with 1 mL of PS particle suspension. Soluble methyl 2-chloropropionate (16 μL from a stock solution of 40 μL in 5 mL of methanol) was added to the reaction solution. The suspension was stirred continuously, and polymerization was allowed to proceed at RT (22 °C) for 24 h. The polymer-grafted PS particles were cleaned by three repeated cycles of centrifugation (10 min for 16000*g*) and resuspension in $NaHSO_3$ solution (50 mM) and water to remove adsorbed copper complexes. Finally, the latex suspension was washed with a 0.1 M EDTA solution three times and with water three times to remove any copper complex remaining within the grafted surface. Glucose-containing glycopolymer layer was grafted on PS NPs using similar procedures. All the grafted structures were characterized in terms of thickness, grafting density, molecular weight, and PDI.

For the synthesis of glycopolymer layers (both glucose and galactose containing) with different grafting densities, we took advantage of the cleavable ester group connecting the surface and the polymer chain (Scheme 1). Time-dependent hydrolysis was performed. Glycopolymer-grafted nanoparticles (150 mg) were first well dispersed in 10.5 mL of Milli Q water. Sodium hydroxide solution (0.2 M, 10.5 mL) was then added to the suspension. A portion of the suspension was removed at different time intervals, neutralized, and washed with water 3 times by a centrifugation and redispersion method. Finally, the particles were collected after centrifugation at 16000*g* and vacuum-dried, after which the weight was determined. We also quantified the amount of polymer released from the NP during the hydrolysis. These data were used to calculate the graft density of polymer chains on the NP surfaces. The amount of polymer cleaved from the surface was determined by injecting the supernatant collected after the cleavage experiments into gel permeation chromatography (GPC) equipped with a calibrated refractive index detector (Optilab T-rEX from Wyatt). By using the software ASTRA 6, we calculated the mass of the cleaved polymer. The grafting density shown in Table 1 is the average of the result from two different approaches.

Grafting of Glycopolymer Layers onto Particles with a Diameter of 33 nm. For the synthesis of glycopolymer layers onto smaller particles, ATRP initiator functionalized PS particles were first synthesized from pristine PS particles with a diameter of 27 ± 9.9 nm by surfactant-free seed emulsion polymerization.[35] An aqueous suspension of PS seed latex particles (3 wt %, 0.2 g) was heated to 70 °C with stirring, degassed, and purged with argon. Styrene (225 μL) and 2-(methyl-2′-chloropropionato)ethyl acrylate (106 μL) were added successively to the suspension 10 min apart, and shell polymerization was initiated with potassium persulfate (4 mg in 1.32 mL of water). The reaction was continued for 20 h, after which the latex was cleaned by dialysis against water for 1 week with frequent changes of water. The resultant solid content was determined by thermal gravimetric analysis (TGA) (TGAQ500, TA Instruments). The diameter of the PS particles increased to 36.9 ± 12.8 nm after initiator modification, as determined by dynamic light scattering (Beckman Coulter N4-Plus). Galactose-containing glycopolymer structures were synthesized on these particles by SI-ATRP. Initiator-modified PS particles (100 μL, solid content 6.3 wt %), nonionic surfactant Brij 35 (1.3 mg), and Milli Q water (0.4 mL) were added successively into a glass tube, which was degassed by argon bubbling. To help the PS particles disperse in the water homogeneously, the glass tube was subjected to ultrasonication for 10 min and transferred to the glovebox. In another glass tube, CuCl (6 mg), $CuCl_2$ (1.3 mg), and Me_6TREN (72 μL) were added successively followed by the addition of Milli Q water (6.5 mL). The glass tube was degassed by three freeze−pump−thaw cycles and transferred to the glovebox. 2′-Acrylamidoethyl-β-D-galactopyranoside (50 mg) was added to the prepared solution (0.5 mL). After the dissolution of monomer, the solution was mixed with 0.5 mL of an NP suspension previously prepared. Six microliters of soluble methyl 2-chloropropionate solution (from a stock solution of 40 μL in 5 mL of methanol) was added to the reaction solution immediately. The suspension was stirred continuously, and polymerization was allowed to proceed at RT for 24 h inside the glovebox. The polymer-grafted PS particles were washed by centrifugation/redispersion cycles (with the aid of methanol) with $NaHSO_3$ solution (50 mM) and EDTA solution (100 mM) and water. The solid content was finally determined by TGA.

A glycopolymer layer with lower grafting density was prepared on the particles by adopting a similar procedure except adding 6 mg of the monomer in the polymerization step instead of 50 mg of monomer. We have shown previously that the grafting density of the chains on PS particle surface prepared by SI-ATRP can be reduced by decreasing the monomer concentration.[35]

Synthesis of Poly(*N*-[tris(hydroxymethyl)methyl]acrylamide) Layers with Different Grafting Densities. ATRP initiator modified PS particles of 669 nm was used. The procedure for a typical reaction is presented as follows. In a glass tube, CuCl (6 mg), $CuCl_2$ (1.3 mg), and Me_6TREN (72 μL) were added followed by Milli Q water (6.5 mL). The glass tube was degassed by three freeze−pump−thaw cycles and transferred to the glovebox. *N*-[Tris(hydroxymethyl)methyl]acrylamide (30 mg) was added to this solution (1 mL). After the monomer was dissolved, the solution was mixed with 1 mL of an ATRP initiator modified PS particle suspension that was degassed previously (solid content 6 wt %). Ten microliters of soluble methyl 2-chloropropionate (from a 250 μL stock solution in 5 mL of methanol) was also added to the reaction solution. The suspension was stirred continuously, and polymerization was allowed to proceed at RT for 24 h. The polymer-grafted PS particles were cleaned by three repeated cycles of centrifugation and resuspension in $NaHSO_3$ solution (50 mM) and water to remove adsorbed copper

complexes. Finally, the latex suspension was washed with a 0.1 M EDTA solution three times and then with water three times to remove any copper complex remaining within the grafted surface.

PTHMAM brushes with different grafting densities were prepared by hydrolysis in a similar manner to that of glycopolymer layers on the large nanoparticles (669 nm).

Characterization of Polymer-Grafted Nanoparticles. The hydrodynamic diameter of polymer-grafted nanoparticles was measured by a Coulter N4 Plus particle sizer. The particles were dispersed in buffer at a concentration to allow the count rate to fall between 50 000 and 1 000 000 per second. The dry thickness of the grafted polymer layer on the particles before hydrolysis was measured by SEM (Hitachi S-3000N) and calculated based on the following equation:

$$M_l = n \times \rho \times \frac{4}{3}\pi[(r+t)^3 - r^3] \text{ where } n = \frac{M_o}{\rho[(4/3)\pi r^3]} \quad (1)$$

where M_o is the original weight of initiator-modified PS nanoparticles, M_l is the increase in overall weight after polymerization, n is the number of particles, t is the dry thickness of the brush, r is the radius of PS particles, and ρ is the density of the polymer (we assumed the densities of PS and the glycopolymer were equal to 1.0 g/cm^3). The thickness measured by SEM (24.9 $\pm$ 11.4 nm) and calculated value (23.2 nm) showed good agreement. Because the dry thickness of the grafted glycopolymer layer is thin, within the resolution of SEM, the reported values for the particles after hydrolysis were calculated by applying the above equation.

The grafting density (σ) of the polymer layer was estimated using the equation

$$\sigma = \frac{(M_l - M_0)/M_n \times N_A}{n \times 4\pi r^2}$$

where N_A is the Avogadro's number and M_n is the molecular weight of the grafted polymer chains. The molecular weight of grafted polymer was obtained by cleaving the polymer chains from the nanoparticles by the hydrolysis of the ester bond under high base condition (3.5 M NaOH for 2 weeks). The supernatant and washings were collected and analyzed by GPC for molecular weight determination.

The smaller nanoparticles grafted with glycopolymer were viewed on a Hitachi H7600 PC-TEM (Hitachi) at an accelerating voltage of 80 kV, and images recorded with an AMT Advantage HR digital CCD camera (Advanced Microscopy Techniques). The grafting density for the glycopolymer layer on the sample nanoparticle was estimated by using the equation $\sigma = (h\rho N_A)/M_n$,[48] where M_n is the molecular weight of free polymer in the solution, N_A is Avogado's number, h is the polymer layer thickness measured by TEM, and ρ is the density of the glycopolymer (we assumed the density of glycopolymer chains is equal to 1 g/cm^3).

The surface area (A) for a given nanoparticle was calculated by $A = n \times 4\pi t_{hydro}^2$ where t_{hydro} is the hydrodynamic radius of polymer-grafted nanoparticles as measured by dynamic light scattering and n is the number of particles, which was correlated by weight (M) through the equation $M = n\rho \times (4/3)r_P^3$ where r_p is the radius of polymer-grafted particles in the dry state. The final equation to calculate the surface area is $A = (M/\rho \times (4/3)r_P^3) \times 4\pi t_{hydro}^2$.

Molecular weights and polydispersities of glycopolymer samples were determined using GPC on a Waters 2690 separation module fitted with a DAWN EOS multiangle laser light scattering detector from Wyatt Technology Corp. with 18 detectors placed at different angles and a refractive index detector (Optilab DSP from Wyatt Technology Corp.). An Ultrahydrogel linear column with a bead size of 6−13 μm (elution range 10^3 to 5 $\times$ 10^6 Da) and an Ultrahydrogel 120 with a bead size of 6 μm (elution range 150 to 5 $\times$ 10^3 Da) from Waters were used. The dn/dc value of soluble galactose polymer and glucose polymer in the mobile phase was determined at λ = 620 nm to be 0.158 and 0.159 mL/g, respectively, and was used for determining molecular weight parameters. The number-average mean square radius moments were taken as the radius of gyration of the polymer.

Biological Analysis. Gelatin veronal buffer (GVB) (without Ca^{2+} and Mg^{2+}), antibody-sensitized sheep erythrocytes (5 $\times$ 10^8 cells/mL), pooled normal human serum, and zymosan were purchased from Complement Technology Inc. (Tyler, TX, USA). Rabbit erythrocytes were collected by drawing 4.5 mL of rabbit blood into a 0.5 mL buffered sodium citrate Vacutainer at the Animal Care Centre, University of British Columbia. Normal human serum was also collected in serum tubes from healthy consenting donors at the Centre for Blood Research, University of British Columbia. The protocol was approved by the University of British Columbia's clinical ethics board. Serum was prepared by allowing the blood to clot for 30 min at room temperature and centrifuging the serum-containing tubes at 1734g for 30 min in an Allegra X-22R centrifuge (Beckman Coulter, Canada).

Complement Activation Analysis by Complement Consumption Assays. Complement consumption was assessed in normal human serum by measuring the residual hemolytic capacity of the complement system after contact with nanoparticles.

Rabbit Erythrocyte Based Hemolytic Assay. The relative capacity of the glycopolymer or PTHMAM-grafted or bare PS nanoparticles to activate complement was studied using NHS. In a 300 μL reaction volume (microfuge tube), nanoparticles (150 cm^2, in 100 μL of GVB) were combined with NHS (150 μL) in GVB (50 μL) containing 0.15 mM Ca^{2+} and 1 mM Mg^{2+}, pH 7.4 (GVB-CM) and were incubated for 30 min at 37 °C. As controls, nanoparticles were replaced by GVB-CM (no complement activation) or the isolated preactivated cell wall from *Saccharomyces cerevisiae* known as zymosan (0.33 μg/μL, full complement activation). Polymers containing residues of glucose, galactose, or PTHMAM were also tested in the absence of nanoparticles for their ability to activate complement. Reaction mixtures were subsequently chilled to 4 °C and subjected to centrifugation at 1500g for 15 min. Resulting serum supernatants (50%) were collected and assessed for residual complement activity using a modified hemolytic assay based on the alternative pathway as described previously.[49] Hemolytic reactions were performed in microtiter (96-well) plates. Each serum reaction was diluted to 2, 3, 4, 6, 8, 10, and 12% in GVB containing 7 mM Mg^{2+} and 10 mM EGTA, pH 7.4 (GVB-ME), and initiated with the addition of rabbit erythrocytes (6.0 $\times$ 10^7 cells/mL, UBC Animal Care Facility) in a final volume of 300 μL. Cells were previously washed three times in GVB and counted using the Advia 120 Hematology System (Siemens, Erlangen, Germany). Hemolytic reactions were incubated at 37 °C for 45 min and stopped with 30 mM EDTA (final concentration), after which unlysed cells were pelleted by centrifugation at 600g, 7 min, RT. Erythrocyte lysis, reflected by the released hemoglobin in the supernatant, was quantified by measuring the absorbance at 405 nm using the Mithras LB 940 microplate reader from Berthold Technologies (Bad Wildbad, Germany). A value for complete cell lysis was provided by a control reaction consisting of rabbit erythrocytes mixed with H_2O. Spontaneous hemolysis in the absence of NHS was subtracted as background. Residual activity of treated serum (*e.g.*, nanoparticle, zymosan, or other reagent) was compared with the residual activity of serum incubated with buffer alone. Percentage of complement consumption by different nanoparticle samples was calculated by subtracting the residual lytic activity from 100%.

Sheep Erythrocyte Based Hemolytic Assay. A modified hemolytic assay was performed to determine the level of complement activation (consumption) by the nanoparticles grafted with glycopolymer or PTHMAM layers. Two incubation steps were utilized. In the first step, glycopolymer- or PTHMAM-grafted PS nanoparticles (50 cm^2, 20 μL) were incubated with 180 μL of GVB-CM-diluted human serum (20% dilution) at 37 °C. After 1 h, the serum-treated PS nanoparticles were centrifuged for 3 min at 5900g, and the serum supernatants were collected and diluted 1:2 in GVB-CM. The diluted supernatant serum was then incubated in equal volume (75 μL) with the antibody-sensitized sheep RBC (EA cells) for 1 h at 37 °C to determine the amount of complement activity remaining in the serum. Heat-aggregated IgG (final concentration 5 mg/mL) was also incubated with GVB-CM-diluted human serum for 1 h at 37 °C and used as the positive control. EDTA (1 mM)-incubated serum was used as a

negative control. All reactions were stopped by the addition of 0.3 mL of GVB-EDTA. Control tubes containing equal volumes of EA cells and GVB-CM buffer (75 μL) were subjected to either GVB-EDTA (20 mM) (negative control), blank control, or dH_2O (100% lysis) control. Intact EA cells were pelleted by centrifugation at 5900*g* for 3 min, and the supernatants were collected. Percentage EA lysis was calculated using average absorbance values as follows: %EA lysis = (A_{540}, test sample − A_{540}, blank)/(A_{540}, 100% lysis − A_{540}, blank) × 100%. Percentage of complement consumption by different nanoparticle samples was expressed as 100% − %EA lysis.

For the soluble polymer, 20 μL of solution (6.1 mg/mL), which has the same amount of polymer as grafted on the particles with a surface area of 50 cm^2, was incubated with 180 μL of GVB-CM-diluted human serum (20% dilution) at 37 °C. The hemolytic assay was performed by the same techniques as with the particles, except that there was no centrifugation step.

Determination of the Pathway of Glc NP Mediated Complement Activation. Normal or immunodepleted (C1q, C2, factor D) human serum (CompTech) was added (50 μL) to Glc 1, Glc 6 (20 μL, 50 cm^2), or HEPES buffer containing 5 mM $CaCl_2$ and 5 mM $MgCl_2$ (20 μL). Samples were incubated at 37 °C for 30 min and subsequently quenched by adding an equal volume (70 μL) of 40 mM EDTA. C2-depleted serum was used to "knock-out" classical and lectin pathway-mediated complement activation, whereas C1q-depleted and factor D-depleted serum were used to "knock-out" classical and alternative pathway-mediated complement activation, respectively. The extent of complement activation in each serum type was determined by measuring C3a levels (Quidel MicroVue C3a Plus ELISA). NHS depleted of certain complement protein was obtained by immunoaffinity chromatography. The product is tested for the absence of certain complement protein by functional assays for different pathway activity or alternative double immunodiffusion, reconstituted with certain complement protein, and retested to verify that a functional classical pathway is restored. More detailed information can be found at the CompTech Web site (http://www.complementtech.com/depletedsera.htm).

C3a and SC5b-9 Levels by Immunoassays. Precalculated surface areas (50 cm^2, 20 μL) of glycopolymer-grafted polystyrene particles were incubated with 180 μL of fresh human serum at 37 °C. After a 1 h incubation, the particle−serum mixture was centrifuged at 5900*g* for 3 min, and C3a and SC5b-9 levels in the serum supernatants were quantified according to the manufacturer's instructions using the Microvue C3a Plus EIA kit and the MicroVue SC5b-9 Plus EIA kit (Quidel, San Diego, CA, USA). Absorbance was measured at 450 nm, and analysis of the assay used a four-parameter curve fit for C3a ELISA and a linear fit for the SC5b-9 ELISA drawn from standard values.

Analysis of Adsorbed Protein Corona on Glycoplolymeric Structures from Serum by Quantitative Mass Spectrometry. *Influence of Conformation of the Glycopolymer Layer.* The composition of the adsorbed protein corona and a quantitative comparison of abundance of proteins on glycopolymer-grafted nanoparticles from serum were determined by mass spectrometry-based proteomic analysis. Glycopolymeric structures with two different graft densities (0.03 and 0.06 chains/nm^2) on PS nanoparticles (669 nm), which yielded completely different complement consumption results, were analyzed. Glycopolymer-grafted PS nanoparticles (45 μL, 113 cm^2) were incubated with 405 μL of fresh human serum at 37 °C for 1 h, after which the nanoparticles were washed three times with 180 μL of PBS buffer. The protein-adsorbed particles were resuspensed in 100 μL of 6 M urea/2 M thiourea (in 10 mM HEPES, pH 8.0), reduced (1 μg of DTT per 50 μg of estimated sample protein for 30 min at RT), alkylated (5 μg of iodoacetamide per 50 μg of sample protein for 30 min at RT), digested with LysC (1 μg/50 μg sample protein for 3 h at RT), diluted 4× with 50 mM NH_4HCO_3, and digested with trypsin (1 μg/50 μg sample protein for 12 h at RT). Peptide mixtures were then analyzed by a Thermo Electron Orbitrap VELOS equipped with an Agilent 1290 HPLC. A combination of fragmentation methods of CID (collision-induced dissociation) and HCD (high-energy collision-induced dissociation) was applied to obtain optimal results.

For proteome profiling by relative quantification, binary analysis was performed by chemical dimethylation of peptides using either light (CH_2O) or medium (CD_2O) isotopologues of formaldehyde as previously described.[50,51] Briefly, samples (trypsin digested) were dissolved in 100 μL of 100 mM TEAB buffer. CH_2O (4 μL, 4%, "light", 0 mM ADP/GDP) or 4% CD_2O ("medium", 0.5 mM ADP/GDP) was added followed by 4 μL of 600 mM $NaBH_3CN$ (light and medium). The mixture was incubated for 1 h at RT, at which point, the reaction was quenched with 16 μL of 1% ammonia (10 μL of NH_4Cl (3.0 M)). Finally, 50 μL of 10% acetic acid was added, and the two differentially labeled samples (pH allowed to stabilize to 3.5 overnight at 4 °C, adding more 20% acetic acid to maintain pH 3.5, then diluted with 200 μL of buffer A) were pooled and desalted using high-capacity STAGE tips made in the MS lab.

Influence of Chemistry of the Glycopolymer Structure. To delineate the difference between carbohydrate structures, a similar mass spectrometry based proteomic analysis was performed using nanoparticles grafted with glucose- and galactose-containing polymers at a grafting density of about 0.03 chains/nm^2.

Statistical Analysis. Results are expressed as mean ± SD (standard deviation) of five independent experiments for the sheep erythrocyte hemolytic assay and three independent experiments for ELISA. Student's *t* test was performed to compare the grafted polymer samples to both the buffer control and bare PS particles. Differences were considered significant when $p < 0.05$.

Conflict of Interest: The authors declare no competing financial interest.

Acknowledgment. The authors acknowledge funding from the Canadian Institutes of Health Research (CIHR) and Natural Sciences and Engineering Research Council (NSERC) of Canada. The authors thank the LMB Macromolecular Hub at the UBC Center for Blood Research for the use of their research facilities. These facilities are supported in part by grants from the Canada Foundation for Innovation and the Michael Smith Foundation for Health Research (MSFHR). The authors also acknowledge support from UBC Bioimaging and UBC Mass Spectrometry Facilities. J.N.K. holds a Career Investigator Scholar award from the MSFHR. J.H.F. is supported by a Banting Fellowship. E.M.C. holds a CSL Behring Research Chair and a Tier 1 Canada Research Chair in Endothelial Cell Biology and is an adjunct Scientist with the Canadian Blood Services. J.N.K. and E.M.C. are members of the University of British Columbia Life Sciences Institute (LSI).

Supporting Information Available: Characterization of glycopolymer- and PTHMAM-grafted nanoparticles, complement activation brought about by different nanoparticles, and the proteomic analysis of the protein corona on different particles. This material is available free of charge *via* the Internet at http://pubs.acs.org.

REFERENCES AND NOTES

1. Kim, B. Y.; Rutka, J. T.; Chan, W. C. Nanomedicine. *N. Engl. J. Med.* **2010**, *363*, 2434–2443.
2. Jain, R. K.; Stylianopoulos, T. Delivering Nanomedicine to Solid Tumors. *Nat. Rev. Clin. Oncol.* **2010**, *7*, 653–664.
3. Bao, G.; Mitragotri, S.; Tong, S. Multifunctional Nanoparticles for Drug Delivery and Molecular Imaging. *Annu. Rev. Biomed. Eng.* **2013**, *15*, 253–282.
4. Nel, A. E.; Mädler, L.; Velegol, D.; Xia, T.; Hoek, E. M.; Somasundaran, P.; Klaessig, F.; Castranova, V.; Thompson, M. Understanding Biophysicochemical Interactions at the Nano-Bio Interface. *Nat. Mater.* **2009**, *8*, 543–557.
5. Monopoli, M. P.; Åberg, C.; Salvati, A.; Dawson, K. A. Biomolecular Coronas Provide the Biological Identity of Nanosized Materials. *Nat. Nanotechnol.* **2012**, *7*, 779–786.
6. Dobrovolskaia, M. A.; McNeil, S. E. Immunological Properties of Engineered Nanomaterials. *Nat. Nanotechnol.* **2007**, *2*, 469–478.
7. Tenzer, S.; Docter, D.; Kuharev, J.; Musyanovych, A.; Fetz, V.; Hecht, R.; Schlenk, F.; Fischer, D.; Kiouptsi, K.; Reinhardt, C.;

Landfester, K.; Schild, H.; Maskos, M.; Knauer, S. K.; Stauber, R. H. Rapid Formation of Plasma Protein Corona Critically Affects Nanoparticle Pathophysiology. *Nat. Nanotechnol.* **2013**, *8*, 772–781.
8. Lundqvist, M.; Stigler, J.; Elia, G.; Lynch, I.; Cedervall, T.; Dawson, K. A. Nanoparticle Size and Surface Properties Determine the Protein Corona with Possible Implications for Biological Impacts. *Proc. Natl. Acad. Sci.* **2008**, *105*, 14265–14270.
9. Walkey, C. D.; Olsen, J. B.; Guo, H.; Emili, A.; Chan, W. C. W. Nanoparticle Size and Surface Chemistry Determine Serum Protein Adsorption and Macrophage Uptake. *J. Am. Chem. Soc.* **2012**, *134*, 2139–2147.
10. Salvador-Morales, C.; Zhang, L. F.; Langer, R.; Farokhzad, O. C. Immunocompatibility Properties of Lipid-Polymer Hybrid Nanoparticles with Heterogeneous Surface Functional Groups. *Biomaterials* **2009**, *30*, 2231–2240.
11. Vonarbourg, A.; Passirani, C.; Saulnier, P.; Benoit, J. P. Parameters Influencing the Stealthiness of Colloidal Drug Delivery Systems. *Biomaterials* **2006**, *27*, 4356–4373.
12. Yang, W.; Zhang, L.; Wang, S. L.; White, A. D.; Jiang, S. Y. Functionalizable and Ultra Stable Nanoparticles Coated with Zwitterionic Poly(carboxybetaine) in Undiluted Blood Serum. *Biomaterials* **2009**, *30*, 5617–5621.
13. Li, A.; Luehmann, H. P.; Sun, G. R.; Samarajeewa, S.; Zou, J.; Zhang, S. Y.; Zhang, F. W.; Welch, M. J.; Liu, Y. J.; Wooley, K. L. Synthesis and *in Vivo* Pharmacokinetic Evaluation of Degradable Shell Cross-Linked Polymer Nanoparticles with Poly(carboxybetaine) *versus* Poly(ethylene glycol) Surface-Grafted Coatings. *ACS Nano* **2012**, *6*, 8970–8982.
14. Hamad, I.; Al-Hanbali, O.; Hunter, A. C.; Rutt, K. J.; Andresen, T. L.; Moghimi, S. M. Distinct Polymer Architecture Mediates Switching of Complement Activation Pathways at the Nanosphere-Serum Interface: Implications for Stealth Nanoparticle Engineering. *ACS Nano* **2010**, *4*, 6629–663.
15. Swartz, M. A.; Hirosue, S.; Hubbell, J. A. Engineering Approaches to Immunotherapy. *Sci. Transl. Med.* **2012**, *4*, 148rv9.
16. Reddy, S. T.; van der Vlies, A. J.; Simeoni, E.; Angeli, V.; Randolph, G. J.; O'Neill, C. P.; Lee, L. K.; Swartz, M. A.; Hubbell, J. A. Exploiting Lymphatic Transport and Complement Activation in Nanoparticle Vaccines. *Nat. Biotechnol.* **2007**, *25*, 1159–1164.
17. Walport, M. J. Advances in Immunology: Complement (first of two parts). *N. Engl. J. Med.* **2001**, *344*, 1058–1066.
18. Passirani, C.; Barratt, G.; Devissaguet, J. P.; Labarre, D. Long-Circulating Nanoparticles Bearing Heparin or Dextran Covalently Bound to Poly(methyl methacrylate). *Pharm. Res.* **1998**, *15*, 1046–1050.
19. Passirani, C.; Barratt, G.; Devissaguet, J. P.; Labarre, D. Interactions of Nanoparticles Bearing Heparin or Dextran Covalently Bound to Poly(methyl methacrylate) with the Complement System. *Life Sci.* **1998**, *62*, 775–785.
20. Sihorkar, V.; Vyas, S. P. Potential of Polysaccharide Anchored Liposomes in Drug Delivery, Targeting and Immunization. *J. Pharm. Pharm. Sci.* **2001**, *4*, 138–158.
21. Wang, H.; Yan, X.; Li, G. L.; Pilz-Allen, C.; Möhwald, H.; Shchukin, D. Sono-Assembly of Highly Biocompatible Polysaccharide Capsules for Hydrophobic Drug Delivery. *Adv. Healthcare Mater.* **2013**, *3*, 825–831.
22. Chauvierre, C.; Labarre, D.; Couvreur, P.; Vauthier, C. Novel Polysaccharide-Decorated Poly(isobutyl cyanoacrylate) Nanoparticles. *Pharm. Res.* **2003**, *20*, 1786–1793.
23. Marques, A. P.; Reis, R. L.; Hunt, J. A. An *in Vivo* Study of the Host Response to Starch-Based Polymers and Composites Subcutaneously Implanted in Rats. *Macromol. Biosci.* **2005**, *5*, 775–785.
24. Thomas, S. N.; van der Vlies, A. J.; O'Neil, C. P.; Reddy, S. T.; Yu, S. S.; Giorgio, T. D.; Swartz, M. A.; Hubbell, J. A. Engineering Complement Activation on Polypropylene Sulfide Vaccine Nanoparticles. *Biomaterials* **2011**, *32*, 2194–2203.
25. Lemarchand, C.; Gref, R.; Passirani, C.; Garcion, E.; Petri, B.; Muller, R.; Costantini, D.; Couvreur, P. Influence of Polysaccharide Coating on the Interactions of Nanoparticles with Biological Systems. *Biomaterials* **2006**, *27*, 108–118.
26. Arima, Y.; Kawagoe, M.; Furuta, M.; Toda, M.; Iwata, H. Effect of Swelling of Poly(vinyl alcohol) Layers on Complement Activation. *Biomaterials* **2010**, *31*, 6926–6933.
27. Bertholon, I.; Vauthier, C.; Labarre, D. Complement Activation by Core-shell Poly(isobutylcyanoacrylate)-polysaccharide Nanoparticles: Influences of Surface Morphology, Length, and Type of Polysaccharide. *Pharm. Res.* **2006**, *23*, 1313–1323.
28. Weinbaum, S.; Tarbell, J. M.; Damiano, E. R. The Structure and Function of the Endothelial Glycocalyx Layer. *Annu. Rev. Biomed. Eng.* **2007**, *9*, 121–167.
29. Ferreira, V. P.; Pangburn, M. K.; Cortes, C. Complement Control Protein Factor H: the Good, the Bad, and the Inadequate. *Mol. Iimmunol.* **2010**, *47*, 2187–2197.
30. Yu, K.; Lai, B. F. L.; Kizhakkedathu, J. N. Carbohydrate Structure Dependent Hemocompatibility of Biomimetic Functional Polymer Brushes on Surfaces. *Adv. Healthcare Mater.* **2012**, *1*, 199–213.
31. Yu, K.; Creagh, A. L.; Haynes, C. A.; Kizhakkedathu, J. N. Lectin Interactions on Surface-Grafted Glycostructures: Influence of the Spatial Distribution of Carbohydrates on the Binding Kinetics and Rupture Forces. *Anal. Chem.* **2013**, *85*, 7786–7793.
32. Yu, K.; Kizhakkedathu, J. N. Synthesis of Functional Polymer Brushes Containing Carbohydrate Residues in the Pyranose Form and Their Specific and Nonspecific Interactions with Proteins. *Biomacromolecules* **2010**, *11*, 3073–3085.
33. Lai, B. F. L.; Creagh, A. L.; Janzen, J.; Haynes, C. A.; Brooks, D. E.; Kizhakkedathu, J. N. The Induction of Thrombus Generation on Nanostructured Neutral Polymer Brush Surfaces. *Biomaterials* **2010**, *31*, 6710–6718.
34. de Gennes, P. G. *Scaling Concepts in Polymer Physics*; Cornell University Press: Ithaca, 1979; pp 25−26.
35. Kizhakkedathu, J. N.; Brooks, D. E. Synthesis of Poly (N,N-dimethylacrylamide) Brushes from Charged Polymeric Surfaces by Aqueous ATRP: Effect of Surface Initiator Concentration. *Macromolecules* **2003**, *36*, 591–598.
36. Arima, Y.; Kawagoe, M.; Toda, M.; Iwata, H. Complement Activation by Polymers Carrying Hydroxyl Groups. *ACS Appl. Mater. Interfaces* **2009**, *1*, 2400–2407.
37. Moghimi, S. M.; Andersen, A. J.; Ahmadvand, D.; Wibroe, P. P.; Andresen, T. L.; Hunter, A. C. Material Properties in Complement Activation. *Adv. Drug Delivery Rev.* **2011**, *63*, 1000–1007.
38. Pedersen, M. B.; Zhou, X. F.; Larsen, E. K. U.; Sorensen, U. S.; Kjems, J.; Nygaard, J. V.; Nyengaard, J. R.; Meyer, R. L.; Boesen, T.; Vorup-Jensen, T. Curvature of Synthetic and Natural Surfaces Is an Important Target Feature in Classical Pathway Complement Activation. *J. Immunol.* **2010**, *184*, 1931–1945.
39. Hariharan, R.; Mays, J.; Russel, W. B. Neutral and Charged Polymer Brushes: A Model Unifying Curvature Effects from Micelles to Flat Surfaces. *Macromolecules* **1997**, *30*, 1787–1792.
40. Dan, N.; Tirrell, M. Polymers Tethered to Curved Interfaces. A Self-Consistent-Field Analysis. *Macromolecules* **1992**, *25*, 2890–2895.
41. Salvati, A.; Pitek, A. S.; Monopoli, M. P.; Prapainop, K.; Bombelli, F. B.; Hristov, D. R.; Kelly, P. M.; Aberg, C.; Mahon, E.; Dawson, K. A. Transferrin-Functionalized Nanoparticles Lose Their Targeting Capabilities When a Biomolecule Corona Adsorbs on the Surface. *Nat. Nanotechnol.* **2013**, *8*, 137–143.
42. Monopoli, M. P.; Bombelli, F. B.; Dawson, K. A. Nanobiotechnology: Nanoparticle Coronas Take Shape. *Nat. Nanotechnol.* **2010**, *6*, 11–12.
43. Lesniak, A.; Salvati, A.; Santos-Martinez, M. J.; Radomski, M. W.; Dawson, K. A.; Aberg, C. Nanoparticle Adhesion to the Cell Membrane and Its Effect on Nanoparticle Uptake Efficiency. *J. Am. Chem. Soc.* **2013**, *135*, 1438–1444.
44. Milani, S.; Bombelli, F. B.; Pitek, A. S.; Dawson, K. A.; Radler, J. Reversible *versus* Irreversible Binding of Transferrin to Polystyrene Nanoparticles: Soft and Hard Corona. *ACS Nano* **2012**, *6*, 2532–2541.

45. Torreira, E.; Tortajada, A.; Montes, T.; de Cordoba, S. R.; Llorca, O. 3D Structure of the C3bB Complex Provides Insights into the Activation and Regulation of the Complement Alternative Pathway Convertase. *Proc. Natl. Acad. Sci.* **2009**, *106*, 882–887.
46. Wu, J.; Wu, Y. Q.; Ricklin, D.; Janssen, B. J. C.; Lambris, J. D.; Gros, P. Structure of Complement Fragment C3b-Factor H and Implications for Host Protection by Complement Regulators. *Nat. Immunol.* **2009**, *10*, 728–733.
47. Kizhakkedathu, J. N.; Norris-Jones, R.; Brooks, D. E. Synthesis of Well-Defined Environmentally Responsive Polymer Brushes by Aqueous ATRP. *Macromolecules* **2004**, *37*, 734–743.
48. Luzinov, I.; Julthongpiput, D.; Malz, H.; Pionteck, J.; Tsukruk, V. V. Polystyrene Layers Grafted to Epoxy-Modified Silicon Surfaces. *Macromolecules* **2000**, *33*, 1043–1048.
49. Morgan, B. P. Measurement of Complement Hemolytic Activity, Generation of Complement-Depleted Sera, and Production of Hemolytic Intermediates. *Methods Mol. Biol.* **2000**, *150*, 61–71.
50. Boersema, P. J.; Aye, T. T.; van Veen, T. A. B.; Heck, A. J. R.; Mohammed, S. Triplex Protein Quantification Based on Stable Isotope Labeling by Peptide Dimethylation Applied to Cell and Tissue Lysates. *Proteomics* **2008**, *8*, 4624–4632.
51. Chan, Q. W. T.; Foster, L. J. Changes in Protein Expression During Honey Bee Larval Development. *Genome Biol.* **2008**, *9*, R156.1–R156.14.
52. Ishihama, Y.; Oda, Y.; Tabata, T.; Sato, T.; Nagasu, T.; Rappsilber, J.; Mann, M. Exponentially Modified Protein Abundance Index (emPAI) for Estimation of Absolute Protein Amount in Proteomics by the Number of Sequenced Peptides per Protein. *Mol. Cell. Proteomics* **2005**, *4*, 1265–1272.